Recombination effects in the structure function evolution at low x. Can they be observed at HERA?

K. Golec-Biernat [a], M.W. Krasny [b], S. Riess [c]

[a] *Dept. of Theoretical Physics, Institute of Nuclear Physics, ul Radzikowskiego 152, 31-342 Kraków, Poland*
[b] *L.P.N.H.E, IN2P3-CNRS, Universities Paris VI et VII, 4, pl. Jussieu, T33 RdC, 75252 Paris Cedex 05, France
and High Energy Physics Lab., Institute of Nuclear Physics, PL-30055 Kraków, Poland*
[c] *II. Institut for Experimental Physics, University of Hamburg, Luruper Chaussee 149, 22761 Hamburg, Germany*

Abstract

Can the non-linear QCD effects resulting from parton recombination be detected at HERA by the H1 and ZEUS detectors? We argue that an extension of the low x domain of the proton structure function F_2 measurements to small electron scattering angle is essential before they can be ruled out. If, on the other hand, they are large, we find that their magnitude cannot be determined unambiguously from the measured Q^2 and x dependence of F_2. This is due to large correlations between the size of recombination effects and the gluon distribution which is very weakly constrained at low x by the F_2 evolution.

1. Introduction

The precision measurement of the deep-inelastic nucleon structure functions in the low Bjorken x region at HERA is expected to provide a novel testing ground for perturbative QCD. The rise of the structure function F_2 at low x, observed by the H1 and Zeus collaborations [1], indicates that the parton recombination processes [2], expected to show up in the dense parton system, may indeed be observed and confronted with perturbative QCD predictions.

However, we find that the present F_2 measurements are not precise enough to either confirm or exclude the presence of parton recombination processes. Consequently, large ambiguities exist in the interpretation of these measurements in terms of parton densities at low x.

In this paper we address the question of whether the presently operating HERA detectors will be capable of resolving the parton recombination effects in the future. We argue that an extension of the measurement domain towards smaller values of the scattered electron angle is indispensable.

In our studies we use simulated data corresponding to our best knowledge on limits of the accuracy which can be achieved after several years of experience in measuring F_2 at HERA.

We analyze these "data" using a program [3], which fits partonic distributions to F_2 data using evolution equations containing parton recombination terms. This is the basic difference of our approach compared with the previous phenomenological studies of parton recombination effects [4], in which fixed parton distribution parametrizations were used.

This paper is organized as follows. In Section 2 we recall the non-linear QCD evolution equations. The

simulated F_2 data are discussed in Section 3. These data are used in the non-linear QCD fits presented in Section 4 and discussed in Section 5. Ambiguities in determining the gluon distribution from data are pointed out in Section 6.

2. The evolution equations

Mueller and Qiu [5] proposed that recombination effects in the QCD evolution equations for parton distributions should be included by adding non-linear terms to the Altarelli–Parisi equations. The form of these terms is controversial [6]. Nevertheless, it is worthwhile to test their validity with forthcoming HERA data. In this paper we use the form of these equations given in [7]:

$$Q^2 \frac{\partial [xg(x,Q^2)]}{\partial Q^2} = P_{gg} \otimes g + P_{gq} \otimes q_s$$

$$- \frac{81\alpha_s^2(Q^2)}{16 R^2 Q^2} \theta(x_0 - x) \int_x^{x_0} \frac{dz}{z} \{zg(z,Q^2)\}^2 \quad (1)$$

$$Q^2 \frac{\partial [xq_s(x,Q^2)]}{\partial Q^2} = P_{qg} \otimes g + P_{qq} \otimes q_s$$

$$- \frac{27\alpha_s^2(Q^2)}{160 R^2 Q^2} \theta(x_0 - x)\{xg(x,Q^2)\}^2$$

$$+ \frac{\alpha_s(Q^2)}{\pi Q^2} \theta(x_0 - x) \int_x^{x_0} dz\{\frac{x}{z}\gamma(\frac{x}{z})G_H(z,Q^2)\},$$

$$(2)$$

where $q_s(x,Q^2)$ and $g(x,Q^2)$ denote the sea quark and gluon distributions, respectively, and G_H satisfies

$$Q^2 \frac{\partial [xG_H(x,Q^2)]}{\partial Q^2}$$

$$= -\frac{81\alpha_s^2(Q^2)}{16 R^2} \theta(x_0 - x) \int_x^{x_0} \frac{dz}{z} \{zg(z,Q^2)\}^2.$$

$$(3)$$

The parameter R, which determines the magnitude of the non-linear terms, corresponds to a transverse size of the region within which the partons (mostly gluons) are concentrated. For $R = 5$ GeV^{-1} (proton radius) partons are uniformly distributed within the

proton, whereas for $R < 5$ GeV^{-1} they are concentrated in clusters of smaller size ("hot spots").

The solution of Eqs. (1)–(3) depends on two parameters: Λ_{QCD} and R, as well as on the form of the parton distributions at the initial scale Q_0^2.

Eqs. (1)–(3) can be solved numerically. We have written a program [3], which solves the equations using the expansion of the parton densities in terms of Chebyshev polynomials. This program was used in the analysis presented below.

3. The simulated data

As we shall see later, the recombination effects represented by the non-linear terms in Eqs. (1)–(3) cannot be identified using recently published H1 and Zeus F_2 data [1]. This is due both to the limited acceptance of the detectors in the low x region and to a large systematic uncertainty of the measurements. The limited angular coverage of the H1 and ZEUS detectors for measuring deep inelastically scattered electrons ($\theta_e \geq 7.5°$) restricts severely the small x domain, where the nonlinear terms of Eqs. (1)–(3) are expected to be important. In addition, the substantial photoproduction background restricts the available y range of the measurement to $y \leq 0.6$.

The measurement domain might be extended towards very small x, of the order 10^{-5}, in a dedicated low x experiment. If the HERMES electron spectrometer [8] were used in a colliding mode in which 30 GeV electrons were scattered off 820 GeV protons accelerated at HERA, a precision measurement of F_2 in this x region would be possible [9] by extending the θ_e domain down to $\theta_e \approx 3°$.

Can the recombination effects be resolved if such dedicated measurement is made? To answer this question we have considered two distinct scenarios of the size of recombination effects and simulated the measurement of the two corresponding F_2 data sets in the angular domain of $\theta_e > 3°$ and $Q^2 \geq 2$ GeV^2. The first data set, called hereafter R_∞, was simulated according to Eqs. (1)–(3) with the non-linear terms omitted (the R parameter was set to infinity) while the second, called hereafter R_3, corresponds to the R parameter set to 3 GeV^{-1}. We then examine if we can unambiguously identify the effects which we have put in from the results of the QCD fits to these two data sets. The

simulated data correspond to an integrated luminosity of 10 pb^{-1}, and to our best knowledge of the limits of systematic accuracy which might be achieved after several years of of experience in measuring F_2.

Both data sets were generated to be compatible with the data published by H1 and ZEUS in the region accessible by the experiments (Figs. 1a and 1b). The error bars are taken to be the anticipated statistical and systematic errors added in quadrature. The systematic errors include an uncertainty in the measured scattered electron momentum and its angle. They are in the range between 5–10%.

4. The QCD fits

To see if the simulated recombination effects can be unambiguously detected, we performed QCD fits to the two data sets using Eqs. (1)–(3). The χ^2 of the fits is defined as the following sum over measured points

$$\chi^2 = \sum_i \frac{(F_2^{\mathrm{exp}}(x_i, Q_i^2) - F_2^{\mathrm{fit}}(x_i, Q_i^2))^2}{\sigma_{i,\mathrm{sys}}^2 + \sigma_{i,\mathrm{stat}}^2} , \qquad (4)$$

where F_2^{exp} and F_2^{fit} are experimental (simulated) and calculated proton structure functions, respectively, and $\sigma_{i,\mathrm{sys}}^2$ and $\sigma_{i,\mathrm{stat}}^2$ are the systematic and statistical errors.

The χ^2 was minimized with respect to the fit parameters using the MINUIT package [10]. The following general form, motivated by the phenomenological studies in the small x region [7], was assumed for the x dependence of the gluon and sea quark distributions at $Q_0^2 = 4$ GeV^2:

$$xg(x) = (A_g \, x^{-\lambda_g} + B_g) \, W_g(x) \qquad (5)$$

$$xq_s(x) = (A_s \, x^{-\lambda_s} + B_s) \, W_s(x) . \qquad (6)$$

$W_{g,s}(x)$ are polynomials whose parameters are not sensitive to the small x behavior of the parton densities. Only the parameters λ, A, B are important in the small x region, and they were fitted.

For simplicity, the magnitude of the R and Λ_{QCD} parameters were fixed in all fits. Λ_{QCD} was taken to be to be 200 MeV (for 4 flavors), which is an average value obtained from the leading log analysis of fixed target DIS experiments [11]. Three values of R were assumed, $R = 3, 5, \infty$ GeV^{-1}. For each minimization step, the momentum sum rule was imposed. We

performed the fits for two values of the angular cut-off of $\theta_e \geq 3°$ and $\theta_e \geq 7.5°$, corresponding to the two detector configurations mentioned above. In all fits the leading log approximation for the linear part of Eqs. (1)–(3) was used.

As a basic consistency check of our procedure, we verified that for each simulated data set we find the parameter values assumed in the data simulation, i.e. a fit to the R_∞ data set leads to a very large value of R, and a fit to R_3 data set finds $R = 3$ GeV^{-1}. The results of these fits are presented in Fig. 1.

5. The recombination effects

In this section we shall interpret the simulated F_2 data by analysing the results of the fits explained in the previous section. Since we know the underlying physics picture of the simulated data sets we can verify if our interpretation is correct and unambiguous.

From the fitted F_2 we extract the logarithmic slopes $\partial F_2 / \partial \log(Q^2)$ for different x values, and compare them for a compact illustration of the fit quality to the logarithmic slopes of the simulated structure function F_2. The results are shown in Fig. 2.

Fig. 2a shows the slopes for R_∞ data set simulated with the minimal detection angle $\theta_e > 7.5°$. Three independent fits to these data were performed: the standard fit with the linear Altarelli–Parisi equations ($R = \infty$ in Eqs. (1)–(3)), and with the parameter R set to $R = 5$ and 3 GeV^{-1} in the fits. In all cases acceptable χ^2 values are obtained ($\chi^2/\mathrm{NDF} = (80, 71, 79)/74$, respectively). Thus, we conclude that the present HERA experiments cannot resolve the recombination effects corresponding to $R = 5$ and 3 GeV^{-1}.

Extending the electron detection angle to $\theta_e > 3°$, and therefore measuring smaller values of x changes the picture considerably as shown in Fig. 2b. Again fits with R set to $3, 5, \infty$ GeV^{-1} were made to the R_∞ data set, but simulated now down to $\theta_e = 3°$. The fit with the linear evolution equations ($R = \infty$) describes the data well ($\chi^2/\mathrm{NDF} = 106/118$) while the $R = 5$ and $R = 3$ fits yield unacceptable χ^2/NDF of $160/118$ and $293/118$, respectively. Thus, we fail to obtain acceptable fits for the $R = \infty$ data set using non-linear evolution equations with $R \leq 5$GeV^{-1}.
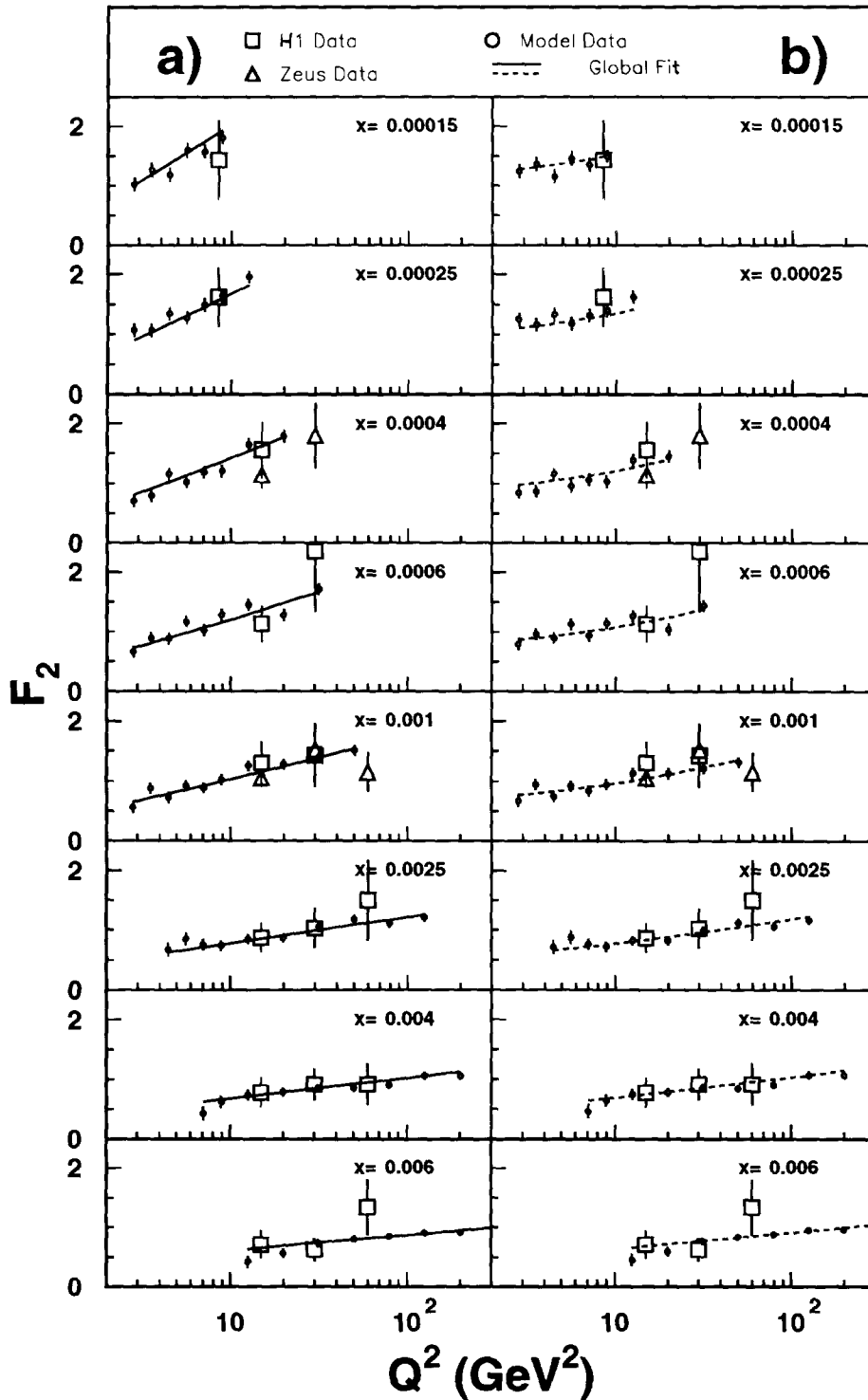
We now reverse the problem and ask if the re-

Fig. 1. Comparison of simulated (open circles) R_∞ (a) and R_3 (b) data on F_2 (for the description see Section 3) to the measured F_2 structure function of H1 (squares) and ZEUS (triangles) [1]. The solid lines represent the $R = \infty$ fit, while the dashed lines $R = 3$ fit, respectively to R_∞ and R_3 simulated data sets. Note that only the low x simulated data are shown. Higher x data points, no shown in the figure, were also used in the fits.
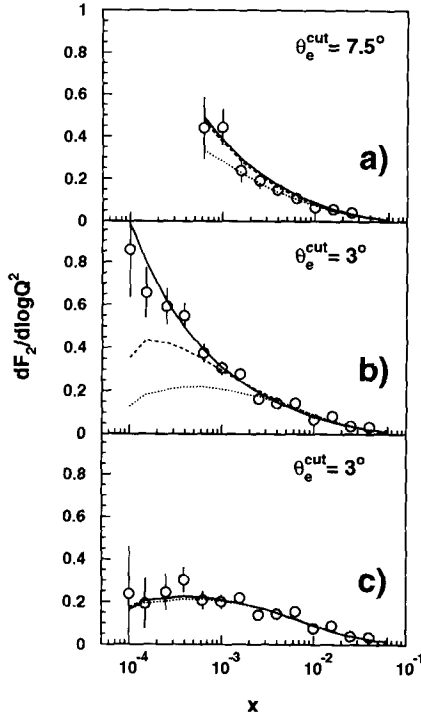
Fig. 2. The F_2 logarithmic slopes $\partial F_2/\partial \log(Q^2)$ as a function of x. The open points represent the values calculated for the R_∞ data set in the domain of $\theta_e > 7.5°$ (a) and $\theta_e > 3°$ (b), and the values calculated for the R_3 data set in the domain of $\theta_e > 3°$ (c). The solid, dashed and dotted lines are derived from the results of the $R = \infty$, 5, 3 GeV^2 fits, respectively.

combination effects present in the R_3 data set can be correctly identified. Fig. 2c shows the slopes derived from the fits to the R_3 data set. Again the larger angular coverage is considered. All three fits, with $R = 3, 5, \infty$ GeV^{-1}, describe this data set equally well ($\chi^2/\text{NDF} = (102, 118, 104/118)$, respectively). As a consequence, if recombination effects are present in the data they cannot be ambiguously detected.

Summarizing, the recombination effects, of the form specified by Eqs. (1)–(3), can be ruled out if they do not exist in the HERA x domain. If they exist their presence could not be confirmed nor their magnitude determined.

6. The gluon distribution at low x

We now examine to which extent the gluon distribution can be constrained at low x if we allow the re-
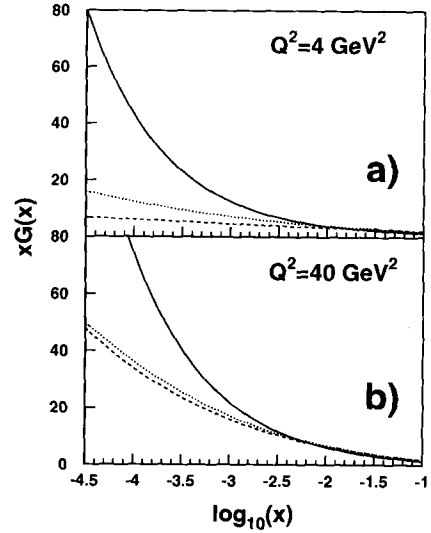

Fig. 3. The gluon distribution $xG(x)$ resulting from the fits: at $Q^2 = 4$ GeV^2 (a), and $Q^2 = 40$ GeV^2 (b). The solid lines represent $R = \infty$ fit to the R_∞ data set, the dashed lines represent $R = \infty$ fit to the R_3 data set, and the dotted lines represent $R = 3$ fit to the R_3 data set simulated in the $\vartheta_e > 3°$ region.

combination terms to be present in the evolution equations.

In Figs. 3a and 3b we show the gluon distributions at $Q^2 = 4$ and $Q^2 = 40$ obtained from the fits of: the linear part of Eqs. (1)–(3) to the R_∞ data set (solid line), the linear part of the Eqs. (1)–(3) to the R_3 data set (dashed line), complete Eqs. (1)–(3) with $R = 3$ GeV^{-1} to the R_3 data set (dotted line).

All fits are of equally good quality. The resulting gluon distributions differ, however, as shown in Fig. 3. These distributions illustrate the uncertainty range of the gluon distribution due to shadowing terms of Eqs. (1)–(3). This uncertainty is particularly large at low Q^2 and, as expected, decreases at large Q^2 where the recombination effects are smaller. The three gluon distributions behave at $Q^2 = 4$ GeV^2 as $x^{-0.5}$, $x^{-0.25}$ and $x^{0.0}$ respectively at small x.

The above analysis indicates clearly that pinning down experimentally the size of the recombination effects is necessary to determine the gluon distribution at low x from the scaling violation of F_2 only.

As our two data sets are compatible with the F_2 data of H1 and ZEUS the above uncertainty is present in the gluon distribution presented in [12].

7. Conclusions

To rule out the presence of the non-linear terms in the QCD evolution equations for the proton structure function F_2 which describe the recombination of partons at low x, we have demonstrated that it is necessary at HERA to detect electrons at smaller scattering angle (below 7.5°) to be sensitive to recombination of partons clustering on a distance scale $R \leq 5$ GeV^{-1}. This could possibly be achieved by means of a precision electron spectrometer, similar to that under construction for the HERMES experiment at HERA but run in colliding mode with 820 GeV protons rather than a gas jet target.

If clustering and recombination effects are important at HERA, and if they are described by the non-linear parts of Eqs. (1)–(3), then their manifestation in F_2 measurements may be mimicked by a suitable choice of the gluon distribution parameterisation at fixed Q_o^2 and conventional linear evolution. Thus, it is essential to measure the gluon distribution by other independent means such as from measurements of σ_L/σ_T, heavy quark production or jet production, if clustering and recombination effects are to be observed unambiguously at HERA.

This analysis has assumed that a leading logarithm approximation is valid for the linear part of Eqs. (1)–(3). Any modifications to these conclusions by making a next-to-leading logarithm approximation and by replacing protons in the HERA storage rings by heavy ions will be reported in separate papers.

References

[1] H1 Collaboration (I. Abt et al.), Nucl. Phys. B 407 (1993) 515;
ZEUS Collaboration (M. Derrick et al.), Phys. Lett. B 306 (1993) 412.
[2] L.N. Gribov, E.M. Levin and M.G. Ryskin, Phys. Rep. 100 (1983) 1.
[3] K. Golec-Biernat, M.W. Krasny and S. Riess, FITEQ–Users Guide (in preparation).
[4] J. Bartels, K. Charchula and J. Feltesse, Proceedings of the Workshop "Physics at Hera", Hamburg 1991, p. 193;
A. Altman, M. Gluck and E. Reya, Phys. Lett. B 285 (1992) 359.
[5] A.H. Mueller and J. Qiu, Nucl. Phys. B 268 (1986) 427.
[6] J. Bartels and M.G. Ryskin, Z. Phys C 60 (1993) 751.
[7] J. Kwieciński, A.D. Martin, W.J. Stirling and R.G. Roberts D 42 (1990) 3645.
[8] HERMES Collaboration, Technical Design Report, DESY, 1993.
[9] M.W. Krasny, Saclay Note, Nov. 1991, unpublished.
[10] F. James and M. Roos, MINUIT–Users Guide, Program Library D 506, CERN, 1981.
[11] BCDMS Collaboration (A.C. Benvenuti et al.), Phys. Lett. B 223 (1989) 490.
[12] H1 Collaboration (I. Abt et al.), Phys. Lett. B 321 (1993) 161.